ALEPH 98-012
CONF 98-002
February 27 , 1998

P R E L I M I N A R Y

Isolated photons and constraints on Trilinear Gauge WWγ couplings at LEP2

ALEPH Collaboration

Contact person: Agnieszka Jacholkowska (Agnieszka.Jacholkowska@cern.ch)

Abstract

A study of single and multiphoton events has been performed for the data sample obtained with the ALEPH detector at 161,172 and 183 GeV in 1996 and 1997. The anomalous coupling parameters are measured, leading to the preliminary values:

$$\Delta\kappa_\gamma = 0.05\ ^{+1.2}_{-1.1}(\text{stat})\ \pm 0.3(\text{syst})$$

$$\lambda_\gamma\ = -0.05\ ^{+1.6}_{-1.5}(\text{stat})\ \pm 0.3(\text{syst})$$

These results are in agreement with Standard Model expectations for the WWγ trilinear coupling parameters.

ALEPH contribution to 1998 conferences

1 Introduction

The study of the reaction $e^+e^- \to \gamma(\gamma) + \mathrm{X}$ (where X represents undetectable particles) at LEP2 energies covers a wide range of physics topics [1]. An inclusive measurement of neutral events with at least two energetic photons is a test, at these energies, of the purely QED process $e^+e^- \to \gamma\gamma(\gamma)$, and of the pointlike structure of the electron. One may search for pairs of neutral SUSY particles such as neutralinos (followed by their decay into a gravitino and a photon) [2]. When a final state leads to the $\nu\overline{\nu}\gamma(\gamma)$ channel, it comprises the radiative return to the Z with one or several photons (the Z decaying into $\nu\overline{\nu}$), the W exchange in the t-channel, and also the W exchange with a photon coupled to the W.

The latest process gives access to the trilinear gauge boson WWγ vertex, which can be described by three independant C- and P-conserving parameters $\mathrm{g}_1^\gamma, \kappa_\gamma, \lambda_\gamma$. Traditionnally these parameters are referred to as "anomalous", as they are related to the following W boson properties:

$$\begin{aligned} \text{charge} \quad & \mathrm{Q_w} = e\mathrm{g}_1^\gamma \\ \text{magnetic dipole moment} \quad & \mu_\mathrm{w} = \frac{e}{2\mathrm{m_w}}(\mathrm{g}_1^\gamma + \kappa_\gamma + \lambda_\gamma) \\ \text{electric quadrupole moment} \quad & \mathrm{q_w} = -\frac{e}{\mathrm{m_w^2}}(\kappa_\gamma - \lambda_\gamma) \end{aligned}$$

In the Standard Model (SM), for real photons these parameters take the values:

$$\mathrm{g}_1^\gamma = 1 \ , \ \kappa_\gamma = 1 \text{ and } \lambda_\gamma = 0.$$

In this paper, instead of κ_γ the deviation from the SM will be used: $\Delta\kappa_\gamma = \kappa_\gamma - 1$.

The corresponding parameters for WWZ couplings are currently studied in W pair production analyses together with those for the WWγ vertex [3]. In this channel a minimal set of 5 independant parameters is necessary, and usually a model-dependance is introduced to reduce this set to at most 3 of them (e.g. the model with the parameters $\alpha_W, \alpha_{W\phi}, \alpha_{B\phi}$ [3]). The $\nu\overline{\nu}\gamma(\gamma)$ channel offers less sensitivity than the W pair production channel, but is complementary with respect to the measurement of κ_γ. Moreover, an observation of an excess of high energy photons (far above the Z peak energy) would correspond directly to anomalous contributions to the WWγ vertex due to New Physics beyond the SM.

This paper describes the measurement of the anomalous coupling parameters $\Delta\kappa_\gamma$ and λ_γ from the $e^+e^- \to \nu\overline{\nu}\gamma(\gamma)$ channel, using data taken at 161,172 and 181 $\to$ 184 GeV. The theoretical framework of this study follows the one presented in [4],[5] and [6], in which the matrix elements of the standard and non-standard couplings are calculated using the helicity formalism. The results obtained contribute to the gauge coupling measurements together with the W pair and single W production channels.

2 The ALEPH detector

The ALEPH detector and its performance are described in detail in [7, 8]. Here is given only a brief description of the properties which are relevant to the present

analysis.

The central part of the ALEPH detector is dedicated to the reconstruction of the trajectories of charged particles. Following a charged particle from the interaction point outwards, the trajectory is measured by a two-layer silicon strip vertex detector, a cylindrical drift chamber and a large time projection chamber (TPC). The three tracking detectors are immersed in a 1.5 T axial field provided by a superconducting solenoidal coil.

The electromagnetic calorimeter (ECAL) is situated between the TPC and the coil. It is a highly granular lead–proportional-wire sampling calorimeter with a total thickness of 22 radiation lengths and yields a resolution of $\delta E/E = 0.18/\sqrt{E}$, with E in GeV. Photons are identified by their transverse and longitudinal shower profiles in ECAL and the absence of any associated reconstructed charged track.

The iron return yoke is equipped with 23 layers of streamer tubes and forms the hadron calorimeter (HCAL). Combined with ECAL it provides a relative energy resolution of charged and neutral hadrons of $0.85/\sqrt{E}$. Muons are distinguished from hadrons by their distinct pattern in HCAL and by the muon chambers composed of two layers of streamer tubes outside HCAL.

The information from the tracking detectors and the calorimeters are combined in an energy flow algorithm [8]. For each event, the algorithm provides a set of charged and neutral reconstructed particles, called energy flow objects, which are used in the analysis.

3 Event samples and selection

The data have been collected with the ALEPH detector at LEP in 1996 and 1997, at centre of mass energy of 161,172 and 181 $\rightarrow$ 184 GeV; the corresponding luminosities are given in Table 1.

3.1 Selections and cuts

Only events having no charged tracks and at least one photon with an energy $E_\gamma > 0.1\sqrt{s}$ GeV are considered. At most 1 hit is accepted in the muon chambers, to eliminate beam-related and cosmic background events. The loss of candidate events with noisy muon chambers was estimated from random triggers to be 3%; the corresponding correction factor was included in the selection efficiency calculation. The timing of the energy deposition in the ECAL is checked to be consistent with the beam crossing time. This selection removes all photon conversions in the beam pipe or in the material of the tracking devices.

A photon candidate is then identified as a localised energy deposition in the electromagnetic calorimeter with a profile consistent with that of an electromagnetic shower. The additional selections are based on the results of the energy flow algorithm. All events containing more than 0.5 GeV of deposited energy within a cone of 14° with respect to the beam axis are rejected, which removes radiative Bhabha events. The correction factor coming from this cut was estimated from random triggers to be 3.5% and included in the selection efficiency calculation.

Furthermore, to minimize the remaining background, the resulting total energy flow E_{flow} is required to satisfy the condition:

$$10\text{GeV} < E_{flow} < \sqrt{s}/2$$

and to come mostly from photon candidates:

$$|E_{flow} - \sum_i E_\gamma^i| < 2.5 \text{ GeV},$$

where the sum runs over all photons.

The photon energy E_γ is estimated from the electromagnetic energy deposition, correcting for clustering and for electronic readout effects in the data sample. The energy deposited in the HCAL is corrected for the e/π ratio and added to E_γ if the photon points to a crack of the electromagnetic calorimeter. Photon candidates with a leakage in the HCAL are accepted only if $E_{had}/E_\gamma < 10\%$. The consistency between the energy measured from the ECAL pads and from the ECAL wires is also checked.

At least one photon candidate is required to fulfil the following conditions:

$$\theta_\gamma > 20^\circ$$
$$x_T = p_{T\gamma}/E_{beam} > 0.10$$

In addition, for the multiphoton candidates, the energy of the second photon is required to be greater than $0.05\sqrt{s}$, and the overall missing momentum $p_{T_{miss}}$ is required to fulfil the condition: $p_{T_{miss}} > 12\text{GeV/c}$. The last cut removes possible radiative Bhabha events.

Table 1 shows the data and Monte Carlo event samples used in this analysis. The number of selected events agree with the numbers expected from the SM cross-sections determined with the KORALZ Monte Carlo. The cross-section measured from the data at 183 GeV, with the present analysis, is 3.45 ± 0.30 pb, to be compared to the SM prediction of 3.40 ± 0.02 pb.

Table 1: Data and Monte Carlo samples

Energy (GeV)	Luminosity (pb^{-1})	Data N Events	Monte Carlo N Events
161	11.0	37	2×10^4
172	10.7	31	6×10^4
$181 \rightarrow 184$	58.1	148	8×10^4
Total	79.8	216	16×10^4

3.2 Monte Carlo simulation with KORALZ

The simulation uses a modified version of the KORALZ program [9], which comprises SM expectations (with electroweak corrections) as well as QED radiative corrections, and the contributions of anomalous coupling amplitudes with exact matrix element

calculations [10]. The overall higher order QED correction factor is about 1.4, depending on the centre of mass energy.

To obtain a description of the anomalous couplings in the simulation, each event is assigned a weight which is a function of $\Delta\kappa_\gamma$ and λ_γ. This method provides the lowest error, as the statistical error affects only the differences between the distributions produced from the Standard Model and the ones from "anomalous" matrix elements.

As the matrix element is linear in $\Delta\kappa_\gamma$ and λ_γ:

$$A = A_{SM} + \Delta\kappa_\gamma A_1 + \lambda_\gamma A_2$$

where A_1 and A_2 are the "anomalous" amplitudes, the cross-section and the differential distributions are bilinear forms of $\Delta\kappa_\gamma$ and λ_γ. For each event it is thus sufficient to store weights for only six configurations in the $(\Delta\kappa_\gamma, \lambda_\gamma)$ plane, in order to compute any cross section or kinematic variable as a function of $\Delta\kappa_\gamma$ and λ_γ. Therefore only one simulation is necessary for a given centre of mass energy. The procedure of introducing the couplings at the level of the leading order amplitudes is discussed in [10] and [11].

3.3 Kinematic regions used in this study

Two kinematic variables of the photon are used in the fit: the photon polar angle θ_γ and the scaled energy $\mathrm{x_E} = \mathrm{E}_\gamma/\mathrm{E}_{\mathrm{beam}}$. Two regions of interest are used, below and above the Z peak, the sensitivity to anomalous couplings being very poor in the Z peak region:

Table 2: Number of events (N Events) entering the fit in the two kinematic regions, and corresponding Monte Carlo samples. The number of expected events is estimated from the KORALZ cross-sections, corrected by the acceptance factors. .

Kinematic region	N Events, Cross section fit seen	(expected)	N Events, $(\mathrm{x_E}, \theta)$ fit	N Events, Monte Carlo
Reg. 1 : $x_E < 0.67$	93	(101.0)	60	$\sim 10^4$
Reg. 2 : $x_E > 0.76$	30	(32.8)	18	$\sim 10^4$

- region (1) where $\mathrm{x_E} < 0.67$, corresponding to the photon energy:

$$\mathrm{E}_\gamma < \mathrm{E}_\gamma(\mathrm{Z}^0) - 3\Gamma_\mathrm{Z}$$
$$\text{where } \mathrm{E}_\gamma(\mathrm{Z}^0) = (\mathrm{s} - \mathrm{m}_\mathrm{z}^2)/2\sqrt{\mathrm{s}}$$

  is the expected photon energy in case of one photon radiative return. In this region, an angular cut $|\cos\theta_\gamma| < 0.94$ is performed to select events for the cross section fit, and $|\cos\theta_\gamma| < 0.90$ for the differential distributions; this cut

has been optimised for the sensitivity and the number of events used in the fit.

- region (2) where $x_E > 0.76$, corresponding to:

$$E_\gamma > E_\gamma(Z^0) + 0.5 \text{ GeV}$$

In this region, an angular cut $|\cos\theta_\gamma| < 0.94$ is performed to select events for the cross section fit, and $|\cos\theta_\gamma| < 0.82$ for the differential distributions.

The cut values vary slightly with the centre of mass energy. Table 2 shows the number of events used in the fit procedure for each kinematic region.

Figure 1 shows the distribution of the scaled energy and $|\cos\theta_\gamma|$ for data, compared to the Standard Model predictions. A good compatibility is observed for both variables. In the following analysis, the two kinematic regions were treated separately and the results merged at the level of the likelihood functions.

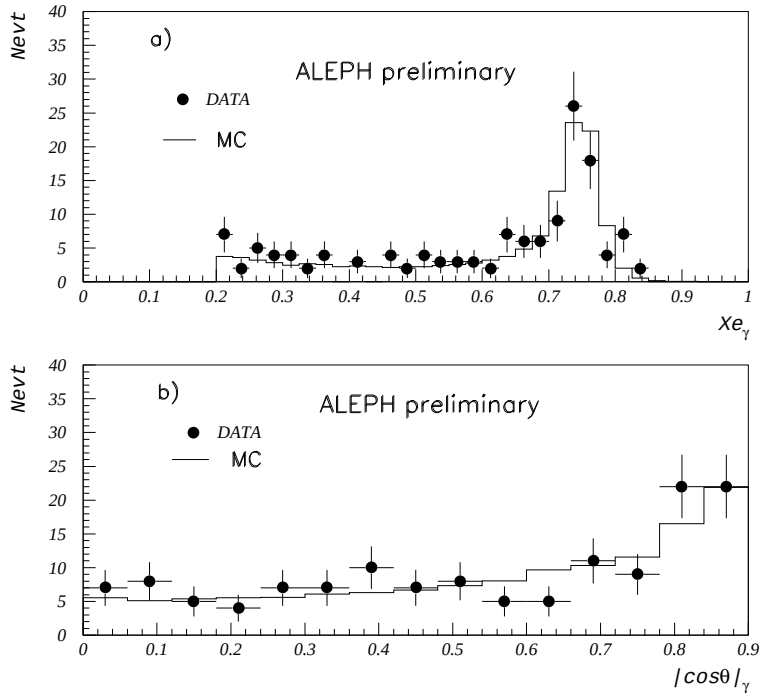

Figure 1: Distribution of a) the scaled energy x_E and b) the absolute value of the cosine of the polar angle of single photons, for data and Monte Carlo at 183 GeV.

3.4 Sensitivity to the anomalous couplings

The sensitivity to the anomalous couplings $\Delta\kappa_\gamma$ and λ_γ have been studied using the KORALZ Monte Carlo program.

Figure 2 gives the predicted sensitivity of the cross-sections for both kinematic regions. The estimators are defined for high values of $\Delta\kappa_\gamma$ and λ_γ:

$$S^{\pm}_{\Delta\kappa_\gamma} = \frac{\sigma(\Delta\kappa_\gamma = \pm 10., \lambda_\gamma = 0.)}{\sigma_{SM}} - 1.$$

$$S^{\pm}_{\lambda_\gamma} = \frac{\sigma(\Delta\kappa_\gamma = 0., \lambda_\gamma = \pm 10.)}{\sigma_{SM}} - 1.$$

The cross sections decrease when the centre of mass energy increases; however the sensitivity of the cross sections to the anomalous couplings increases more than linearly between 161 GeV and the highest expected LEP 2 energy.

As an example, Figure 3 gives the sensitivity as a function of x_E at 183 GeV. Here, both kinematic regions are expected to contribute to the $\Delta\kappa_\gamma$ determination whereas λ_γ is sensitive only to the photons above the Z^0 peak.

3.5 Background contributions

The possible contributions to the $e^+e^- \to \gamma(\gamma) + X$ channel, other than $X = \nu\overline{\nu}$, may come from radiative Bhabhas, QED multiphotons or SUSY particles. The angular and energy cuts eliminate the first two contributions. The SUSY particles have not yet been observed, however they could interfere in the anomalous coupling interpretation of the deviations from the Standard Model.

The irreducible background in region 1 comes from the multiphoton Z return.

The KORALZ simulation of higher order effects gives a correction about $+100\%$ for the cross-section in region 1, and about -30% in region 2, thus decreasing the number of observed events..

A theoretical estimate of the error on these correction factors is below 10%. However, only comparisons with complete calculations from the exact matrix elements (not present in KORALZ) for the 2 and 3 hard bremsstrahlung photons will allow a satisfactory estimation of this uncertainty. A discussion of the uncertainty due to the implementation of the matrix elements with anomalous couplings for the multiphoton events will be presented in a future publication [11].

4 Likelihood fit

The limits for anomalous coupling parameters have been derived from the generalised likelihood expression:

$$L = \frac{(N_{th})^{N_{obs}}\, e^{-N_{th}}}{N_{obs}!} \prod_{i=1}^{Nobs} P_i$$

P_i is the probability for each event obtained from the double differential distributions (x_E, θ_γ).

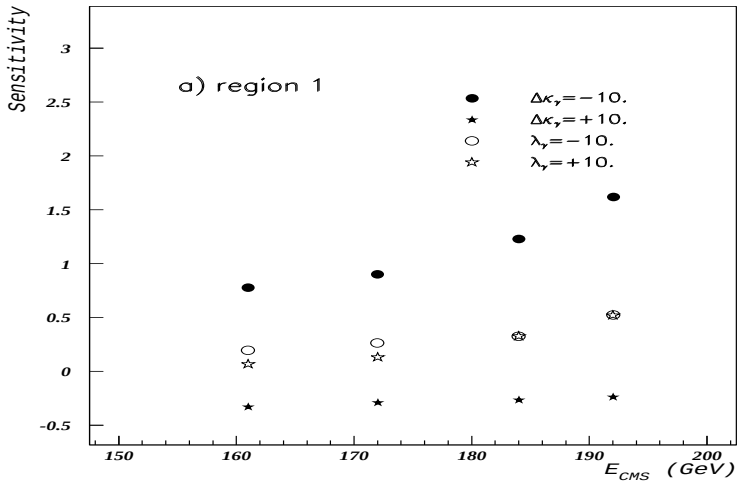

ALEPH preliminary

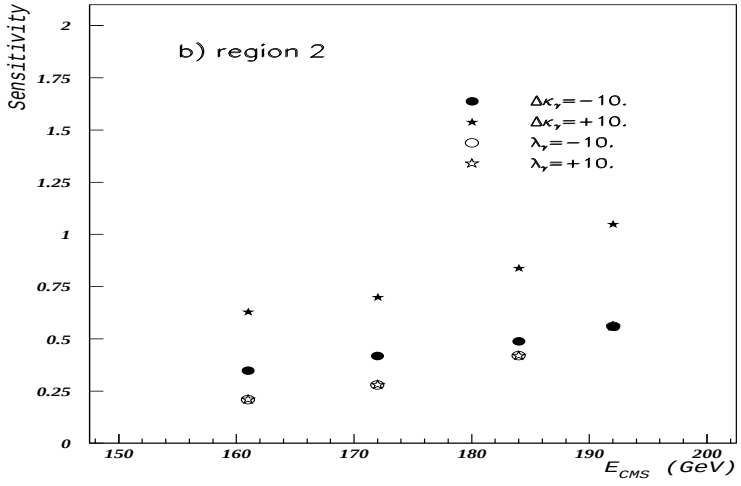

Figure 2: Sensitivity $S^{\pm}_{\Delta\kappa_\gamma}$ and $S^{\pm}_{\lambda_\gamma}$ as defined in the text, as a function of the center of mass energy, for Regions 1 and 2

This likelihood formula contains two parts: the first one concerning the number of observed events, the second one being related to differential distributions for each kinematic region. This leads to an expression containing four terms:

$$\log(\mathrm{L}) = \log(\frac{(\mathrm{N_{th}})^{\mathrm{N^{(1)}_{obs}}}\,\mathrm{e^{-N_{th}}}}{\mathrm{N^{(1)}_{obs}!}}) + \log(\frac{(\mathrm{N_{th}})^{\mathrm{N^{(2)}_{obs}}}\,\mathrm{e^{-N_{th}}}}{\mathrm{N^{(2)}_{obs}!}}) + \sum \log(\mathrm{P^1_i}) + \sum \log(\mathrm{P^2_i})$$

where $\mathrm{N_{th}}$ is the expected number of events in each region, including background:

$$\mathrm{N_{th}} = \mathrm{Luminosity} \times \mathrm{Acceptance}(\Delta\kappa_\gamma, \lambda_\gamma) \times \sigma(\Delta\kappa_\gamma, \lambda_\gamma) + \mathrm{Background}$$

ALEPH preliminary

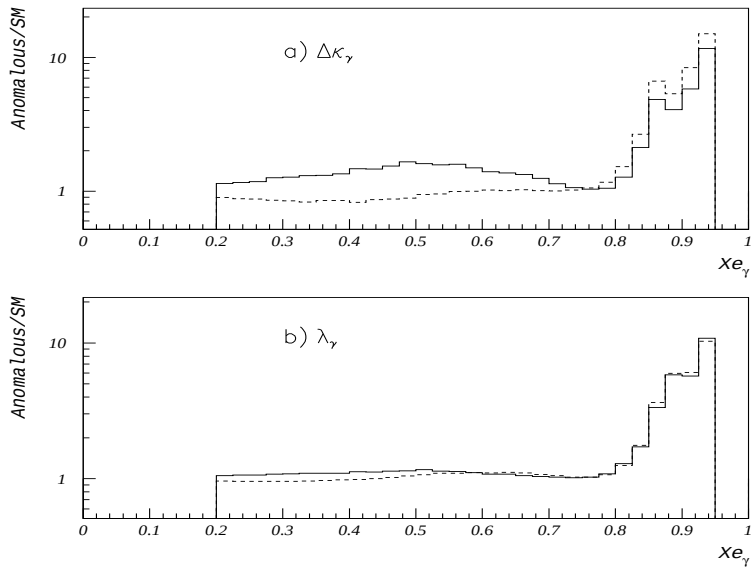

Figure 3: Sensitivity as a function of the scaled energy x_E at 183 GeV centre of mass energy: a) for $\Delta\kappa_\gamma$, b) for λ_γ. Full line (resp. dashed line) is for a parameter value of -10. (resp. +10.).

The acceptance convoluted with the experimental resolution leads to correction factors of 1.10 for the first kinematic region and 0.7 for the second; these correction factors are constant (within $\pm 2\%$) in each region. The trigger efficiency for isolated photons with an energy $> 0.1\sqrt{s}$ is almost 100 %.

The two kinematic regions are treated in almost the same way:

- Region 1 (low energy photons) : the contribution from higher order radiative corrections is described as an almost constant term obtained by the Monte Carlo simulation; this procedure results in a relatively low uncertainty on these corrections. The scaled variable x_E is found to be as discriminant as the angular variable in the fit. Both are used for the $\Delta\kappa_\gamma$ fit, whereas λ_γ is determined only from the cross-section variations.

- Region 2 (high energy photons) : the higher order radiative corrections decrease the number of expected events by 30 %. In this region, the scaled energy x_E is more discriminant than the angular variable, both variables being used in the fit of $\Delta\kappa_\gamma$ and λ_γ. It can be observed that the variation of λ_γ with x_E follows the one of $\Delta\kappa_\gamma$.

It can be shown from the Monte Carlo studies that the cross-sections and distribution shapes vary differently in the two kinematic regions. For low energy photons the "anomalous" effects result from the interference term between the SM amplitude and the "anomalous" amplitude; the resulting variation is monotonous and linear

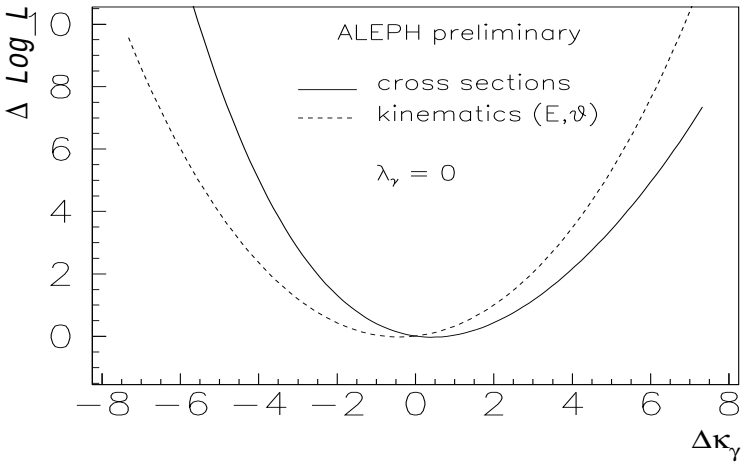

Figure 4: Likelihood curves for the fit of $\Delta\kappa_\gamma$ at $\lambda_\gamma = 0$ for the contribution of the cross-section term (full line) and the distribution term (dashed line).

for $\Delta\kappa_\gamma(\lambda_\gamma) > 0$ and $\Delta\kappa_\gamma(\lambda_\gamma) < 0$ and only one solution is expected for the $\Delta\kappa_\gamma$ and λ_γ fit. For the high energy photons, the variations are quadratic (due to a quadratic contribution of the "anomalous" amplitude) and one or two solutions are expected; the case of one solution corresponds to $\Delta\kappa_\gamma = 0$ or $\lambda_\gamma = 0$. These behaviours have been checked by the use of several samples of Monte Carlo simulated data. The calibration procedure has been used to cross-check the validity of the error given by the likelihood fit. Consistent results have been found for both kinematic regions, as described in Section 6.

5 Results

The log(L) functions have been calculated for the cross-section and distribution terms separately.

Figure 4 shows the -Δlog(L) curves corresponding to the fit of $\Delta\kappa_\gamma$ at $\lambda_\gamma = 0$, the cross-section and distribution contributions being displayed separately. At present energies, the contributions of the cross-section and of the distribution terms are equally important for the fit of $\Delta\kappa_\gamma$. The result for λ_γ is dominated by the sensitivity to the kinematic variation in the second region.

Figure 5 shows the -Δlog(L) functions for $\Delta\kappa_\gamma$ fitted at $\lambda_\gamma = 0$, and for λ_γ fitted at $\Delta\kappa_\gamma = 0$. when the two contributions have been merged.

The results are:

$$\Delta\kappa_\gamma = 0.05\ ^{+1.2}_{-1.1}(\text{stat})\ \text{(assuming } \lambda_\gamma = 0)$$

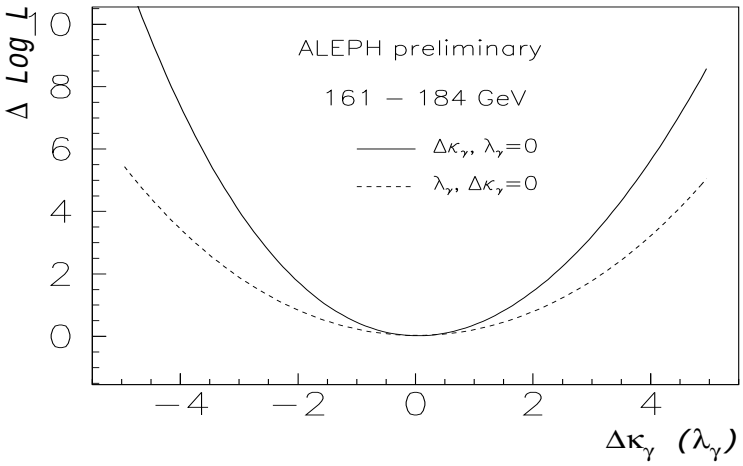

Figure 5: Likelihood curves for the fit of λ_γ at $\Delta\kappa_\gamma = 0$ (full line) and $\Delta\kappa_\gamma$ at $\lambda_\gamma = 0$ (dashed line) for the sum of the cross-section and distribution terms.

$$\lambda_\gamma \ = -0.05 \ ^{+1.6}_{-1.5}(\text{stat}) \text{ (assuming } \Delta\kappa_\gamma = 0).$$

The lower precision for λ_γ is expected as we deal with rather low momentum W's.

The analysis of $\lambda_\gamma(\Delta\kappa_\gamma)$ has been repeated for various values of $\Delta\kappa_\gamma(\lambda_\gamma)$. Figure 6 displays the 1- and $2-\sigma$ contours in the $(\Delta\kappa_\gamma, \lambda_\gamma)$ plane. The results show almost no correlation between the two parameters; this fact reflects the independence of the so-called dipole and quadrupole part of the triple boson interaction.

6 Systematic uncertainties

A total number of 42 simulated Monte Carlo samples have been used to study possible statistical biases due to the very limited data sample. The size of the Monte Carlo samples has been optimized to minimize the inhomogeneity of the weights in the sample: 4 times the data for region 1 and 12 times for region 2. This procedure allows to cross-check the linearity of the measured parameters as a function of the true ones as well as the validity of the errors given by the likelihood fit. Both linearity and error estimations were found to be reliable. The estimation of the possible discrepancy is represented by the fit procedure error.

The contributions to the systematic uncertainty on the determination of $\Delta\kappa_\gamma$ and λ_γ are summarised in Table 3. The total systematic uncertainty is much lower than the statistical one.

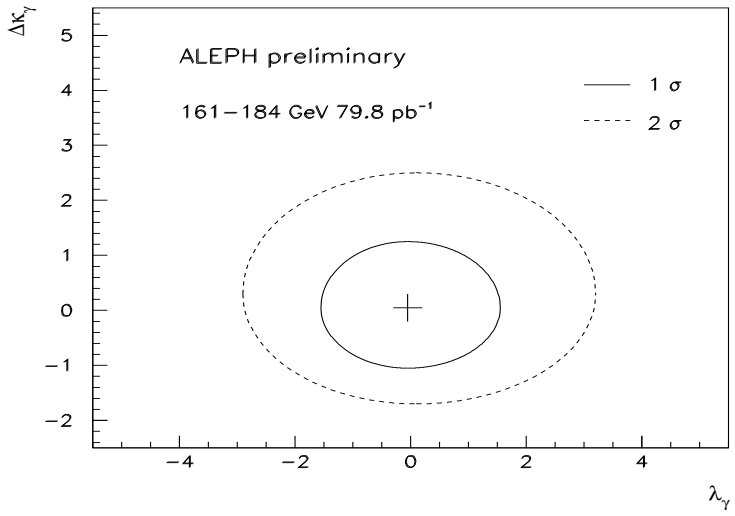

Figure 6: 68% and 95% confidence level contours in the $\Delta\kappa_\gamma, \lambda_\gamma$ plane.

Table 3: Contributions to the systematic uncertainty

Origin of uncertainty	Region 1	Region 2
Acceptance corrections $< 2\%$	± 0.1	± 0.1
Photon energy calibration $\pm 1\%$	± 0.1	± 0.2
Background < 1 event	$+\ 0.1$	$+\ 0.1$
Model uncertainty $< \pm 5\%$	± 0.1	± 0.15
Fit procedure	± 0.05	± 0.05
Luminosity value $\pm 0.6\%$	± 0.03	± 0.03
Total	± 0.3	± 0.3

The main contribution to the systematic error in the present study comes from the energy calibration of high energy photons. Here, the redundancy of the photon energy measurement on the pads and on the wires of the ECAL [7] plays a crucial role. This photon energy calibration can be checked with a large QED photon sample.

The model uncertainty in introducing the anomalous couplings into the simulation has been checked in [11]. The reliability of the simulation of the Standard Model will be addressed in a separate publication. One should notice that the last point will play a crucial role in this analysis when higher statistics will be available. As seen in Figure 1 and Table 2, the present simulation describes well the data.

Another contribution to the uncertainty on the total cross-section part of the fit is given by the luminosity error. The other contributions such as background will

substantially decrease when the luminosity of the data sample increases.

7 Conclusions

The anomalous coupling parameters $\Delta\kappa_\gamma$ and λ_γ have been measured from isolated photon production at 161,172 and 183 GeV. The preliminary results from the fit to the cross-sections and to the energy and angular distributions of the photons are:

$$\Delta\kappa_\gamma = 0.05\ ^{+1.2}_{-1.1}(\text{stat})\ \pm 0.3(\text{syst})$$

$$\lambda_\gamma\ = -0.05\ ^{+1.6}_{-1.5}(\text{stat})\ \pm 0.3(\text{syst})$$

The uncertainty is largely dominated by the limited statistics of the data sample.

In the future, with more data and higher energy, this measurement will provide an independant way of determination of the anomalous couplings, with low systematic uncertainties.

8 Acknowledgements

It is a pleasure to thank the SL division of CERN for the excellent performance of the LEP collider. We would like to thank J.Kalinowski for his help and discussions in the study of the anomalous couplings at LEP2 energies, and Z. Wąs for providing us with a Monte Carlo generator containing the gauge sector for the reaction $e^+e^- \to \nu\overline{\nu}\gamma(\gamma)$.

References

[1] see ref. 6 to 9 from :

ALEPH Collaboration, "A study of single and multi-photon production in e^+e^- collisions at centre-of-mass energies of 130 nd 136 GeV", Phys. Lett. **B 384** (1996) 333.

[2] ALEPH Collaboration, "Searches for supersymmetry in the photon(s) plus missing energy channels at $\sqrt{s} = 161$ GeV and 172 GeV", CERN-PPE-97-122, to be published in Phys. Lett. B.

[3] OPAL collaboration, "Measurement of triple gauge boson couplings from W^+W^- production at $\sqrt{s} = 172$ GeV", CERN-PPE-97-125, to be published in Z. Phys. C

ALEPH collaboration, "Measurement of Triple Gauge-Boson Couplings at 172 GeV", CERN-PPE-97-166, to be published in Phys. Lett. B

[4] G.V. Borisov, V.N. Larin, F.F Tikhonin, *Zeit. Phys.* **C41** (1988) 287.

[5] J. Abragam, J.Kalinowski, P.Sciepko, Phys. Lett. **B 339** (1994) 136.
F. Berends *et al.*, Nucl. Phys. **B 301** (1988) 583.

[6] Physics at LEP2, CERN 96-01, 525 (see references here).

[7] ALEPH Collaboration, "ALEPH: A Detector for Electron-Positron Annihilations at LEP",*Nucl. Instr. Meth.* **A 294** (1990) 121.

[8] ALEPH Collaboration, "Performance of the ALEPH Detector at LEP",*Nucl. Instr. Meth.* **A 360** (1995) 481.

[9] S.Jadach, B.F.L.Ward and Z.Wąs, Comp. Phys. Comm. 79 (1994) 503.

[10] D. Choudhbury, J.Kalinowski MPI-PTH /96-73, IFT-96/17.

[11] A. Jacholkowska, J. Kalinowski and Z.Wąs, to be published in Phys. Lett. A.